Energy for Sustainable Development 41 (2017) 128–138

Contents lists available at ScienceDirect

Energy for Sustainable Development

A general architecture for electric power management of small scale NCRE converters: Design methodology and validation

Franco Hernández [a], Luciano E. Chiang [b,*], Patricio Corbalán [b]

[a] Dept. Electrical Eng., University of Bio-Bio, Chile
[b] Dept. Mechanical & Metallurgical Eng., Pontifical Catholic University of Chile, Chile

ARTICLE INFO

Article history:
Received 6 December 2016
Revised 18 July 2017
Accepted 7 September 2017
Available online xxxx

Keywords:
Small-scale NCRE converters: PM axial flow generator
Programmable buck converter
Multiple NCRE source battery charging

ABSTRACT

A design methodology, its validation and evaluation, for optimal electric energy power management NCRE (NonConventional Renewable Energy) converters used for battery charging is presented, targeting small-scale units (i.e. <10 kW). It is a general-purpose solution that has been tested with different prime movers: river turbine, tidal turbine, wind turbine, and wave energy converter. There are two critical components in the configuration: the electric generator, and the buck converter or MPPT (Maximum Power Point Tracker). The design of these two components must give careful consideration to the behavior of the primary energy source as well as battery charging requirements. The topology selected for the generator is an axial flux generator with permanent magnets, because it allows matching the low optimal speed of the primary energy converters without the use of speed multipliers such as gears and pulleys. The programmable buck converter topology is selected because it can be used both as a voltage or current source, and hence it works well with battery charging,which is a primary application for small-scaleoff-gridNCRE converters. Cost-effectiveness of the solution is achieved by the simple design methods, low cost components and materials, and simple manufacturing methods.

Introduction

The focus of this work is small-scale NCRE (Non Conventional Renewable Energy) conversion. The objective is to provide electric energy to off-grid isolated communities, for domestic or small industrial applications in a sustainable manner. In order to improve economic feasibility it is necessary to increase throughput of existing solutions while at the same time reducing costs. True low-cost reliable solutions are thus necessary to make small scale NCRE conversion a true alternative to the most common solution, which is the use of fossil fuel based generators. Cost effectiveness is taken into account from the beginning in the design process by bearing in mind the following design guidelines: a)low-cost materials, b)simple manufacturing methods, and c)simplified design methods.

Hence, in this work, a customizable low cost architecture is presented for converting NCRE sources such as marine tidal and wave energy, or wind energy, into electric energy stored in batteries at a small-scale level. Some authors define these as systems of <10 kW (Gitano-Briggs, 2010). For practical purposes, it is necessary to store energy for use on a need basis (Arrau, 2016; Chiang-Sánchez, 2012). The problem of energy storage is global because of the variable nature of NCRE sources. This can be addressed by several energy storage means (Beaudin et al., 2010) such as a) Pumped hydro storage, b) Compressed air energy storage, c) Batteries (Lead-acid, Nickel cadmium, Sodium sulfur, Lithium-ion, Zinc bromine, Vanadium redox), d) Superconducting magnetic energy storage, e)Hydrogen storage, e) Flywheels, and f) Capacitors and supercapacitors. The best choice is case dependent.

Studies in Chile show that the most promising NCRE sources are solar and marine energy (Aquatera, 2014). Solar energy conversion has expanded strongly in the last years, pushed vigorously by price reduction in solar panels. However, marine energy contribution, in spite of having an even higher potential (particularly wave energy), lags far behind, and the causes are a mixture of technical and economic issues.

The architecture tested in this work pursues economic sustainability of the electric power generating unit and the power electronics to deliver it. Hence, it differs from other approaches with similar objectives (Bhende et al., 2011) in that the strategy is to prioritize simplicity and reliability.

Micro controller embedded lean software is used to control operation in order to obtain maximum power performance. The same microcontroller and the signals used to control operation also serve to implement a condition monitoring scheme, which is a feature usually present only in large NCRE systems (Rodriguez et al., 2003), but not at the small scale level because of the high cost added. Condition monitoring is a desirable functionality since successful small scale off-grid systems require being almost maintenance free given that access can be extremely difficult and costly.

* Corresponding author.
E-mail address: lchiang@ing.puc.cl (L.E. Chiang).

https://doi.org/10.1016/j.esd.2017.09.001

Nomenclature

A_{o1}	Magnet face area [m^2]
B_R	Remanent Magnetic Field Density of magnet [tesla]
C_{max}	Maximum capacitance for an overdamped response [F]
C_{min}	Minimum capacitance for a desired voltage ripple [F]
ΔI_o	Output current ripple [Amp]
e	Airgap length [m]
ε_{12}	Induced electromagnetic force in a magnetic circuit formed by 2 coils and 2 magnets [V]
ε_F	Induced electromagnetic force in a phase [V]
f	PWM modulation frequency [Hz]
$\varnothing_i$	Magnetic flux through coil i [Weber]
H_c	Magnet Field Coercitivity [Amp/m]
h_c	Radial height of coil core [m]
h_m	Radial height of magnet [m]
I_o	Average output current of buck converter [Amp]
$K_\varnothing$	Generator characteristic constant $\left[\frac{V}{rad/s}\right]$
l_c	Coil depth [m]
l_m	Magnet depth [m]
L	Inductance of buck converter [H]
A_o1	Magnet face area [m^2]
μ_o	Magnetic permeability of air [H/m]
μ	Magnetic permeability of core steel laminations [H/m]
N_c	Number of coils in generator stator
N_m	Number of magnets in generator rotor
N_T	Number of turns in each coil
r_{avg}	Nominal radius of generator [m]
s_c	Pitch between coils [m]
s_m	Pitch between magnets [m]
s_p	Magnet width [m]
T	PWM period [sec]
θ_c	Pitch angle between coils [degree]
θ_m	Pitch angle between magnets [°]
θ_p	Magnet face angle [°]
V_B	Battery voltage [V]
V_T, V_{DC}	Voltage generated by turbine[Volts]
ω_e	Electric angular velocity [rad/s]
ω_m	Mechanical angular velocity [rad/s]

In present day technology, an energy conversion device integrated entirely from third party vendors, will likely face two problems. The first problem is that it would be difficult to find parts from different sources that have matching performance. Second, the separate cost of items when added up would easily exceed the price threshold that tips the scale in favor of fossil fuel based generators. This is why integrated design methods are important because they allow to obtain better results both technical and economical.

Shown in Figs. 1 to 4 are four different NCRE energy converter prototypes designed, built and tested by the authors. Fig. 1 shows a direct drive hydrokinetic tidal turbine with a three phase PM (Permanent Magnet) radial magnetic flow generator built for tidal energy exploitation capable of generating 5KW given a stream velocity of 2 m/s (Arrau, 2016). The advantages of this type of turbines have been discussed in depth by Lago et al. (2010). The design of the blades in this type of rotor is usually based on the Blade Element Momentum theory. The foundations of this method can be found in classical textbooks (Hansen, 2015; Rodriguez et al., 2003).

The authors have developed a software that uses the BEM method to optimize a rotor given the stream velocity, tip and hub radii, and number of blades (Chiang, 2016a). BEM theory also allows estimating forces along the blades, and hence a structural analysis can beperformed. Fig. 2 shows a wave energy converter based on a

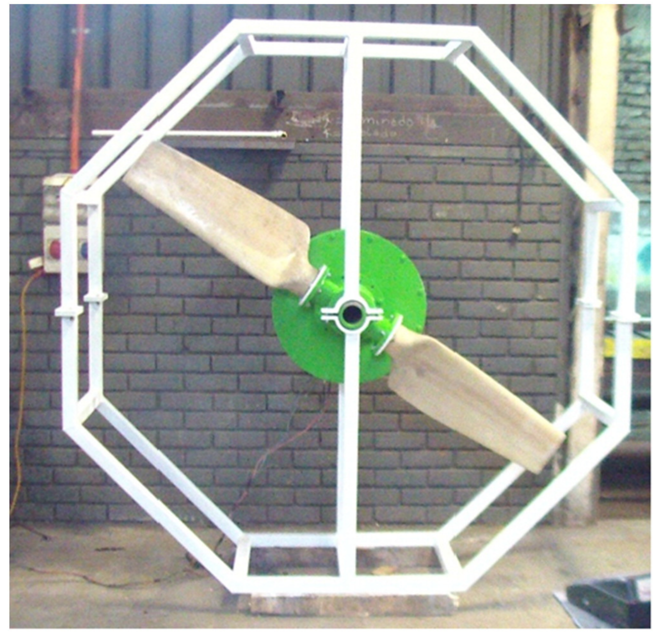

Fig. 1. Tidal turbine (5KW @ 2 m/s stream velocity).

resonant buoy system (Chiang-Sánchez, 2012). The induced resonant relative motion of the submerged buoy and the floating platform feeds in power to the generator unit. Wave energy conversion has great potential, and hence there are many types of wave energy converters being proposed trying to meet expectations not yet fully fulfilled (Drew et al., 2009; Falcao, 2010). Fig. 3 shows a direct drive wind turbine with a two-meter rotor diameter. It uses NACA0012 airfoils and an axial flow three phase permanent magnet generator. Fig. 4 shows a horizontal axis turbine that can be used in small irrigation channels and rivers as well as with marine tides (Muñoz et al., 2014).

The abovementioned NCRE converters have in common that each require a low cost but effective unit management system such as the one discussed herein to connect to the primary converter, and to store and provide electric energy usefully when needed.

In general, the architecture of the NCRE converter should contemplate direct drive from the rotor to the generator. Hence, the generator should be capable of generating enough voltage in the range of 200 to 600 rpm to match the MPP (Maximum Power Point) speed of both wind and water turbines.

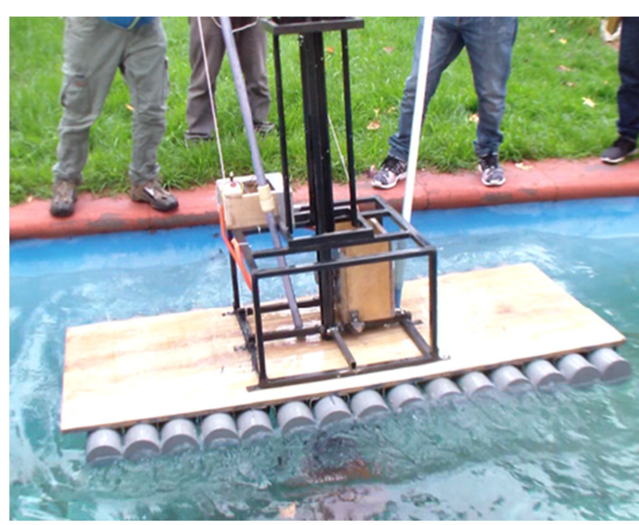

Fig. 2. 100 W Wave energy converter.

Fig. 3. 1 KW Wind turbine @ 6 m/s wind speed.

The electric power unit must work optimally with the NCRE primary source.Previous works (Maalawi and Badr, 2003) consider optimal rotor design methodology as well as overall optimal system design (Ashuri et al., 2014). The authors have developed the Turbem software (Version 2.0; Chiang, 2016a, 2016b) to optimize wind and water kinetic turbines. The Turbem software uses BEM (Blade Element Momentum) theory to obtain the chord length and the twist angle of the optimal blade for a given set of design specifications. In Turbem, the optimization is performed by a mixed gradient search and design space sweepscheme. The turbine rotors shown in Figs. 1, 3 and 4 have been designed and optimized using Turbem (Chiang, 2016a, 2016b, Muñoz et al., 2014).

The remainder of this paper is arranged as follows. In Section2, the proposed architecture is detailed. The generator design methodology is provided in Section3. Section4 details the buck converter circuit. The battery charging methods are described in Section 5. Field test results are provided in Section6 and concluding remarks are made in Section7.

Fig. 4. Tidal turbine tested in an irrigation channel.

Proposed architecture

The variability of the energy source characterizes the input to an NCRE converter. Shown in Fig. 5 is a functional block and energy flow diagram of an NCRE converter. A design methodology, and its validation and evaluation, for the group of system components within the green rectangle is discussed in the sections that follow. The design philosophy is focused toward cost-effectiveness to obtain an economically feasible solution, particularly for regions with low economic development, where these solutions are needed most.

The building blocks of the electric power management architecture that connects to the primary energy converter are the following:

a) A permanent magnet axial flux three-phase generator. This type of generator has advantages over other possibilities such as synchronous generators with field windings, or radial flow permanent magnets generators. Even though they are not as compact in size, axial flux PM generators can generate higher voltages at lower speeds. Important to bear in mind, is that a convenient and almost obligatory feature is that sufficient voltage is generated at low speeds in order to directly match optimal turbine rotor angular velocity. Otherwise, a speed multiplier such as a gearbox will be needed to connect between the turbine and generator shafts, to ensure that both operate at their optimal speeds. The use of a speed multiplier would increase cost and complexity, and this is why as depicted in Fig. 5, a speed multiplier is preferably crossed out. For example, the optimal rotating speed of the turbine shown in Fig. 1 at nominal stream velocity of 2 m/s for maximum power extraction (highest Cp) is in the order of 200 rpm. However, conventional generators usually begin to generate useful voltage (12 V is common for battery charging) at relatively high speeds, for example 800 rpm or more, so they are not a good match for the turbine.
The permanent magnet axial flow generator is an acceptable topology choice that generates useful voltages at low to moderate speeds. The performance of this type of generator is predicted quite accurately using the simplified mathematical model described in this paper. Furthermore, it is easy to build using common available tools, low cost commercial materials, and simple manufacturing techniques (Louie et al., 2012; Louie, 2011; Bumby and Martin, 2005).
b) A three-phase bridge rectifier that converts the three-phase AC output of the generator into a single phase DC output.
c) A configurable buck converter. The DC voltage output of the bridge rectifier is linearly proportional to the generator angular velocity. This velocity is variable because it depends on the constantly changing tide stream velocity as well as in the instantaneous work load in the case of tidal turbines. On the other hand, batteries have a specific charging cycle to follow in order to achieve expected charge efficiency and life cycle duration. To accommodate for a wide range of technologies, sizes and characteristics of existing batteries, the buck converter must be configurable. Furthermore, it must be able to protect the battery as well as the generator from damage, such as overloading for example. Other choices that can be considered for voltage regulation are ON-OFF and PWM modulation. However both are much less efficient than the buck converter, in spite of being simpler.

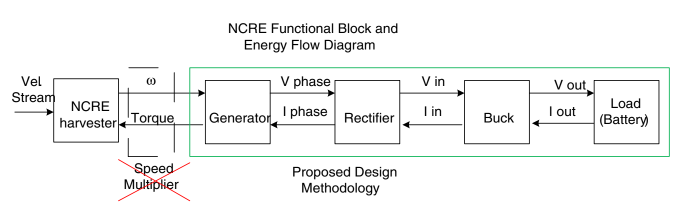

Fig. 5. Functional block and energy flow diagram for an NCRE converter.

d) A bank of batteries. Energy is stored in batteries so it is available on a need basis. Many types of batteries exist, but usually deep cycle batteries are used.

Previous works in NCRE converters have focused largely in connecting and delivering to a three phase electric grid (Bhende et al., 2011) where energy storage is not necessarily a main objective.

A configuration such as presented here is helpful to take full advantage of an NCRE source such as tidal or wave energy. This configuration can be easily extended to other small scale NCRE devices such as wind turbines, hydraulic turbines, and even solar panels. In the latter case, the solar panels can be connected directly to the buck converter as a complementary source of energy.

In order to justify the convenience of the proposed configuration shown in Fig. 5, when compared to other existing commonly used alternatives, we have assembled the following comparative table. Here the main advantages are highlighted and in the following sections the generator and battery charging characteristics of the proposed solution will be discussed in greater detail.

Let us also consider that stricter environmental regulation tendencies make it increasingly difficult to implement large energy projects. This results in cost increments that are usually absent in technical evaluations. Hence, in many places a more plausible strategy is the deployment of small-scale NCRE generation with small units sparsely distributed geographically, giving consideration not only to direct economic issues but also to the fact that because of their lower environmental impact, they are better received by communities (Hiremath et al., 2009; Palit and Chaurey, 2011). As Anyi and Kirke (2011) point out, low cost and simple manufacturing methods of NCRE converters, apart from economic advantages also generate many social benefits for remote communities.

Generator design methodology

Generator architecture

A main building block of the discussed architecture is the permanent magnet axial flux three-phase generator. This topology has important advantages for small scale energy devices as indicated in Table 1, with high torque density, easily adjustable Voltage constant, simple design methodology, low cost of materials, and flexible fabrication methods available. The potential of this generator topology for small NCRE devices has been recognized by many authors and there are continuous efforts toward its improvement (Topaloglu et al., 2016; Probst et al., 2011; Vansompel et al., 2010; Holmes et al., 2005).

In the example shown in Figs. 6, 7 and 8, this particular rotor contains 14 N35 magnets of 13 mm x19 mm face dimensions and a depth of 3 mm. There are 12 copper coils in the stator. The three phases are arranged in a Y connection, each phase connecting 4 coils in series. Each coil in the stator has 70 turns of AWG 18 copper magnet wire.

The main components of the generator are based in low cost materials and simple manufacturing methods. This is an important advantage of the axial flux topology, because it does not require high precision manufacturing. Apart from using commonly available materials, critical parts can be fabricated using conventional machine tools such as lathes, bandsaws, and bench drills.

Both the stator and rotor are covered with layers of epoxy resin and fiberglass for protection.

Generator mathematical model

Fig. 9 is a schematic that is used to model the output of the generator based on magnetic circuit theory (Chiang, 2016b). Using this approach,

Table 1
Comparison of main characteristics of proposed configuration tested in three NCRE devices.

Subsystem	Typical horizontal axis tidal turbine	Typical small wind turbine	Typical wave energy converter (heaving buoy configuration)	Proposed configuration	Advantages of proposed configuration
Mechanical input transmission	Usually speed amplification is required to match marine rotor speed to generator optimal speed	Usually speed amplification is required to match input rotor speed to generator optimal speed	Usually speed amplification is required to match input rotor speed to generator optimal speed.	Direct Drive 1:1 Rack and pinion in case of wave energy converter	Fewer mechanical parts, hence lower risk of mechanical failure. Lower cost. Less vibrations. No wearable parts. Mechanical transmissions with speed amplification have wearable parts.
Generator configuration	Radial flux permanent magnet or synchronous generator with field winding	Radial flux permanent magnet or synchronous generator with field winding)	Linear Array Permanent Magnet Configuration	Axial flux permanent magnet	Axial flow configuration generates higher voltages at lower speeds. Higher torque density Works better in the range of optimal input speed of wind, hydrokinetic, and wave converters, which is relatively low (below 400 rpm in our case). Permanent magnet radial flow configurations usually require high rotating speeds to generate usable voltages (above 800 rpm). Generators based on linear permanent magnet arrays require high linear speeds to obtain usable voltages. Voltage constant of the generator can be easily adjusted by changing air gap spacing. No wearable parts. The alternative of synchronous generators with field winding has wearable sliding contacts. Simplified Design Methodology as presented in this paper
Battery charging	PWM (pulse width modulation), linear regulators, or pulsed chargers	PWM (Pulse Width Modulation), Linear Regulators, or Pulsed Chargers	PWM (Pulse Width Modulation), Linear Regulators, or Pulsed Chargers	Buck converter with open architecture microcontroller (Arduino)	High Efficiency. Step Down DC-DC capability of buck regulators allows charging with any voltage equal or higher than the battery voltage. On Board diagnostics is possible using reduced set of sensors. Dual purpose use of Programmable buck-converter. Lower EMI emissions. Easy implementation. Simplified design methodology as presented in this paper.

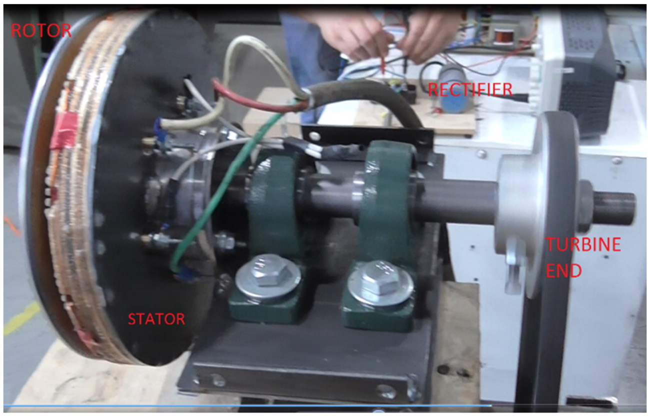

Fig. 6. Three phase 14 permanent magnet/12 coils generator.

with any spreadsheet software, computations are simplified. For design purposes this is convenient since parameter variation can be quickly and easily evaluated and hence optimization can be performed within a reasonable amount of time. Other software tools are available to model this type of generator based on the FEM (Finite Element Method), which may give more accurate results, but nevertheless at the expense of significant more time developing the geometric model and computer run-time (Louie & Szablya, 2011).

To derive the mathematical model let us consider that each pair of coils interacts with a pair of magnets. Magnets and coils are arranged each with different pitches, generating a changing magnetic flow when the rotor spins.

The magnitude of the magnetic flux passing through coils C1 and C2originated by the moving magnets are given by the following expressions according the magnetic circuit theory:

$$\begin{aligned} \varnothing_1 &\approx \frac{H_c l_m}{\frac{H_c l_m}{B_R A_{o1}} + \frac{e}{\mu_o A_{o1}} + \frac{l_c}{\mu A_{o1}}} \\ \varnothing_2 &\approx \frac{H_c l_m}{\frac{H_c l_m}{B_R A_{o2}} + \frac{e}{\mu_o A_{o2}} + \frac{l_c}{\mu A_{o2}}} \end{aligned} \tag{1}$$

Fig. 7. Rotor dish with 14 permanent magnets.

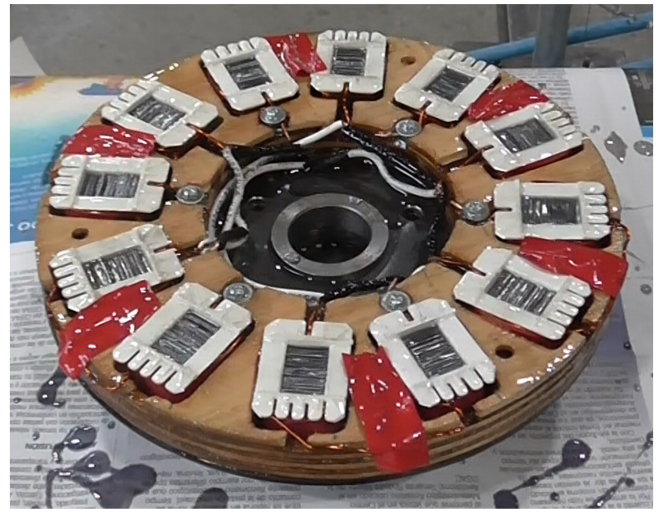

Fig. 8. A 12-coil stator dish.

Geometrically we have.

$$\begin{aligned} h_p &= h_c = h_e \\ s_{o2} &= s_p - (s_c - s_m) \\ A_{o2} &= s_{o2} h_p \\ A_{o2} &= A_{o1}\left(1 - \frac{s_c - s_m}{s_p}\right) \end{aligned} \tag{2}$$

According to Faraday's law, the emf generated in the two coils is:

$$\varepsilon_{12} = N_T \frac{d\varnothing_1}{dt} + N_T \frac{d\varnothing_2}{dt} \tag{3}$$

In practice, the voltage output behaves like a sinusoidal wave as shown in Fig. 10.

Hence,

$$\varepsilon_{12} = N_T \omega_e \left(2 - \frac{s_c - s_m}{s_p}\right) \frac{H_c l_m}{\frac{H_c l_m}{B_R A_{o1}} + \frac{e}{\mu_o A_{o1}} + \frac{l_c}{\mu A_{o1}}} \tag{4}$$

Considering the number of magnets, and coils in each phase, we can estimate the phase voltage magnitude using the following expression:

$$\varepsilon_F = \frac{N_m N_c N_T}{12} \omega_m \left(2 - \frac{s_c - s_m}{s_p}\right) \frac{H_c l_m}{\frac{H_c l_m}{B_R A_{o1}} + \frac{e}{\mu_o A_{o1}} + \frac{l_c}{\mu A_{o1}}} \tag{5}$$

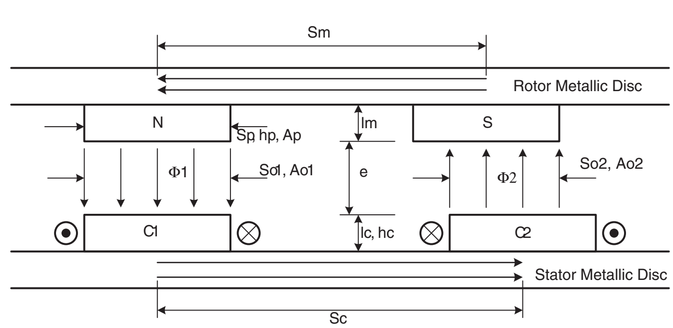

Fig. 9. Magnetic circuit schematics.

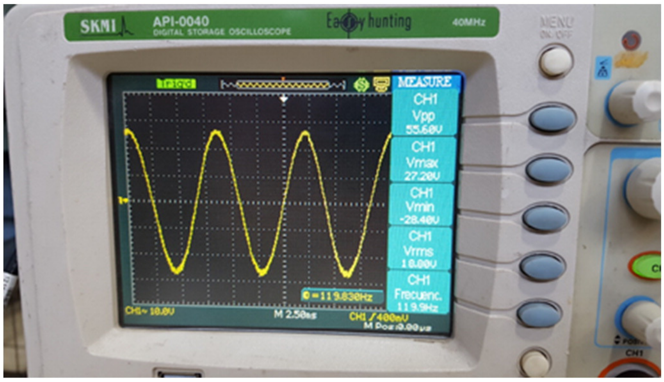

Fig. 10. Phase-to-phase sinusoidal voltage output of PM generator.

If the three phases are connected in Y configuration, and rectified using a 3-phase diode bridge, we obtain the following DC voltage outputestimate:

$$V_{DC} = \frac{\sqrt{3}}{12} N_m N_c N_T \omega_m \left(2 - \frac{s_c - s_m}{s_p}\right) \frac{H_c l_m}{\frac{H_c l_m}{B_R A_{01}} + \frac{e}{\mu_o A_{01}} + \frac{l_c}{\mu A_{01}}} \quad (6)$$

Furthermore, we can estimate the resulting generator constant $K_\varnothing$ as well:

$$K_\varnothing = \frac{\sqrt{3}}{12} N_m N_c N_T \left(2 - \frac{s_c - s_m}{s_p}\right) \frac{H_c l_m}{\frac{H_c l_m}{B_R A_{01}} + \frac{e}{\mu_o A_{01}} + \frac{l_c}{\mu A_{01}}} \quad (7)$$
$$V_{DC} = K_\varnothing \omega_m$$
$$T_G = K_\varnothing i_G$$

Generator calculations

The following are the design variables for the generator built for testing and evaluation shown in Figs. 6–8:

Hence using Eq. (7) we obtain:

$$K_\varnothing = 0.219 \left[{}^{V}/_{rad/s}\right]$$

Table 2
Generation design variables.

Variable	Value
N_m	14
N_c	12
N_T	70
V_T	30
r_{avg} [m]	0.11
H_c [Oersted]	12,000
B_R[Gauss]	12,000
l_m [m]	0.003
e [m]	0.00635
l_c [m]	0.02
θ_c [rad]	0.524
θ_m [rad]	0.449
θ_p [rad]	0.118
h_m [m]	0.019
s_p [m]	0.013
A_{01} [m^2]	0.000247
μ_o [henry/m]	1.25664E-06
μ[henry/m]	0.000628319

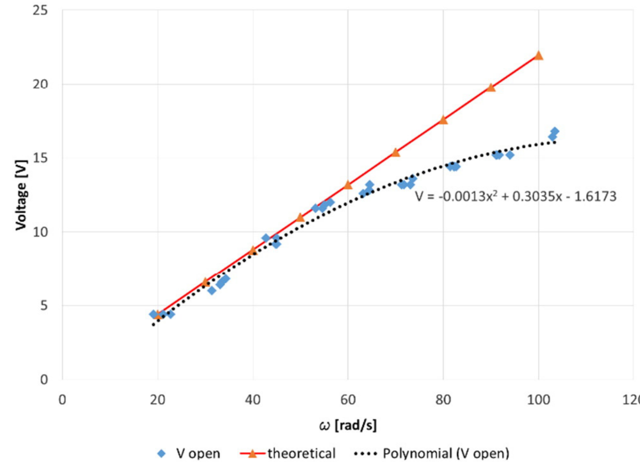

Fig. 11. Voltage vs ω characteristics to obtain Generator Kϕ.

Generator experimental results

To show evidence of the results obtained with the proposed configuration and design methodology, the characteristic curve for the generator of Table 2 is given in Fig. 11, compared to the theoretical predictions.

In this particular generator, a deviation between the measured and predicted voltage output becomes noticeable above 65 rad/s as seen in Fig. 11. This may be caused by the level of vibration that was seen to increase at high angular speed. However this particular generator is intended to run at <35 rad/s and in that range the generator operates quite smoothly. When the generator is connected to a resistive load the behavior shown in Fig. 12 was measured.

As expected, the current does not follow a strictly linear behavior with respect to the angular velocity because the inductive effect in the rotor coils generates higher impedance at higher speeds. Also, as expected, the current magnitude is higher for lower resistive loads. The internal phase-phase resistance is 3.5 Ω and the phase-phase inductance is 0.01H.

Buck converter

The buck converter is another main building block of the proposed configuration. It is governed by an Arduino Uno microcontroller (Arduino, 2016a). This type of controller is very popular among

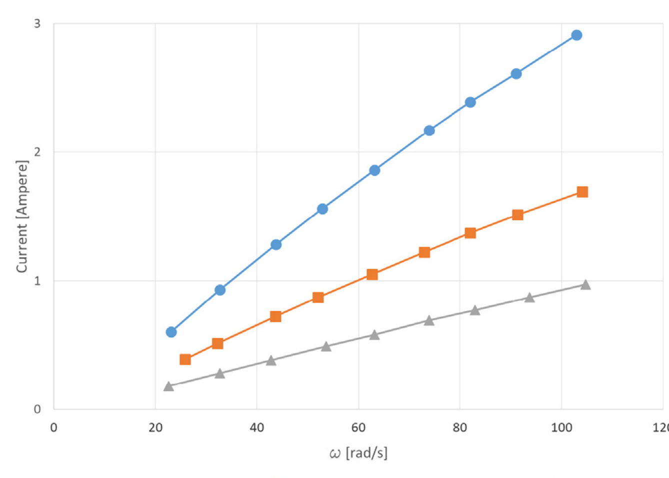

Fig. 12. Current vs ω curves for different resistive loads.

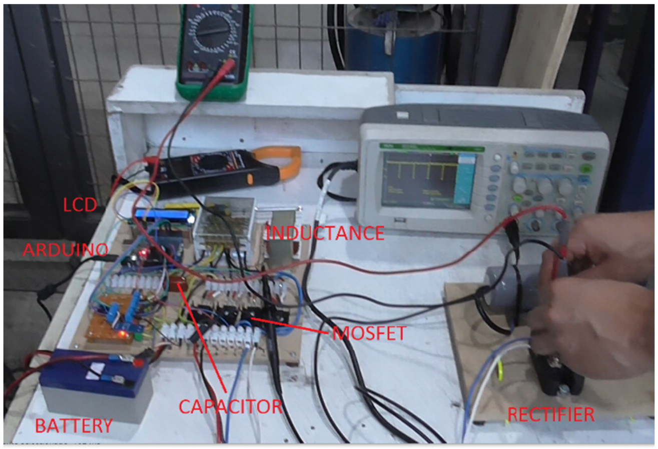

Fig. 13. Configurable buck converter.

developers. It belongs to an open source family of low cost and widely used controllers, and there is ample support in the internet for applications. Furthermore, there are support boards known as shields commercially available that add functionality for a variety of purposes at affordable prices.

A piggy back data logger shield is added in this application, which provides apart from basic data acquisition functionality, higher level functionality such a condition monitoring capabilities. The data logger features allow storing the time history of operating variables on a µSD card for later processing or for setting alarms to take immediate action in case of emergency. The possibility of saving the time history of the operating variables allow monitoring their evolution. If deviation from permissible intervals is detected, alarms are set off for proper actions to be taken.

Buck converter mathematical model

Fig. 14 shows the detailed model of the buck converter shown in Fig. 13. The feedback to maintain constant output voltage is generated by the Arduino based software.

The output voltage V_o is read by analog port 0. The input voltage V_T to the buck converter is read by analog port 1. The output current I_o is read by analog port 2 via a current sensor. The duty cycle D signal is provided by Pin 5. Note that by default the PWM frequency in pin 5 of the Arduino is fixed to 976 Hz, but this value can be modified by changing the scaler of the associated Timer-Counter (Arduino, 2016b). The value of duty cycle D is set continuously, essentially using proportional control to maintain the output voltage V_o and I_o within prescribed ranges. If connected to solar photovoltaic panels the unit power management behaves exactly like an MPPT for charging batteries.

Buck converter computations

The idealized circuit in Fig. 15 is used for specifying the main components of the bulk converter. The derivation and discussion of equations can be found in a variety of texts (Lázaro-Blanco & Barrado-Bautista, 2007).

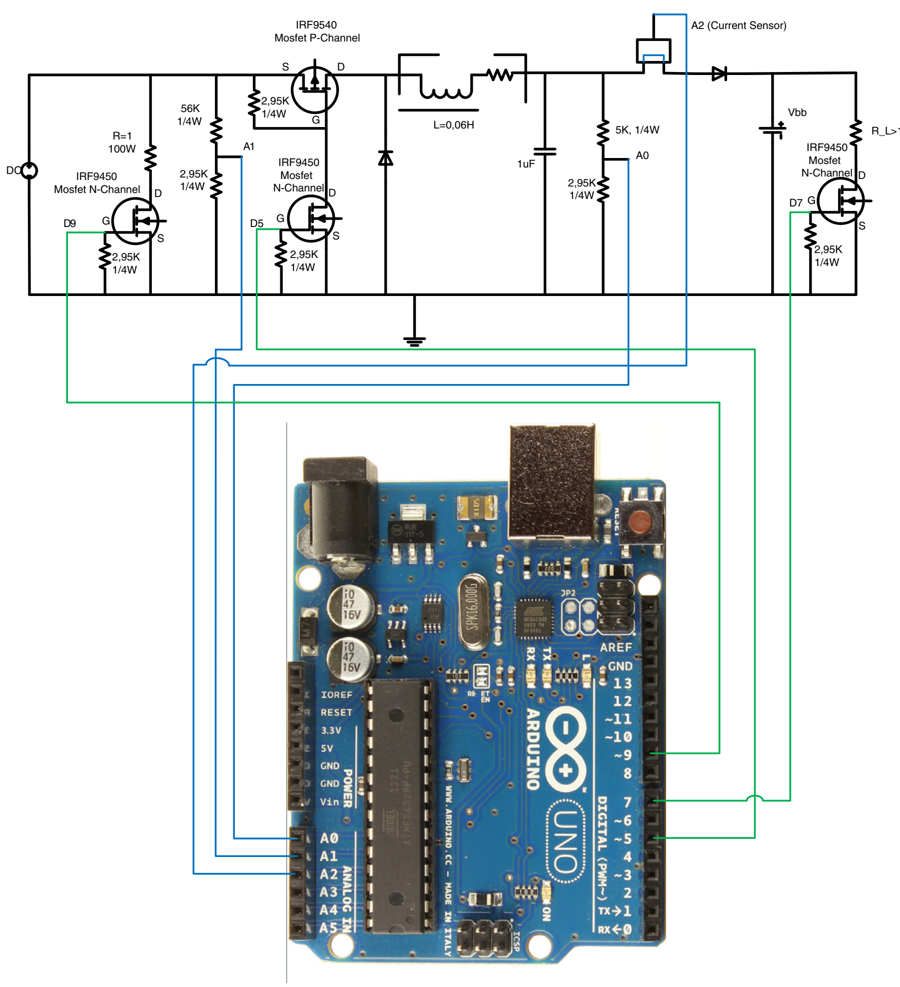

Fig. 14. Detailed buck converter schematics.

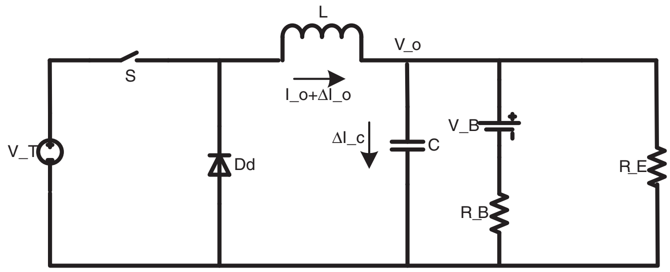

Fig. 15. Basic buck converter model.

The following are the simplified classical equations and conditions that govern the operation of this circuit.

The PWM duty cycle D is given by:

$$D = \frac{T_{On}}{T_{On} + T_{Off}} = \frac{T_{On}}{T} \quad (8)$$

But also

$$D = \frac{V_o}{V_T} \quad (9)$$

The expected output current ripple is given by

$$\Delta I_o = \frac{(V_T - V_o)D}{f \cdot L} \quad (10)$$

The following expression governs the output voltage ripple ΔV_0, giving the minimum capacitance necessary to reach this ripple value.

$$C_{\min} = \frac{\Delta I_0}{8 \cdot f \cdot \Delta V_0} \quad (11)$$

On the other hand, an overdamped current response is desired. For this purpose, the maximum value of the capacitor is the following, so that the system poles are real and negative.

$$C_{\max} = \frac{L}{4}\left(\frac{1}{R_B} + \frac{1}{R_E}\right)^2 \quad (12)$$

In order to select the proper values of L and C for the buck converter circuit, we propose the following sequence of calculations:

Given the values of V_o,I_o and V_T for the application,

a) Select convenient values of L and f (i.e. highest possible). For example, set L according to the largest inductance you can build and mount within the available space.
b) Compute value of expected ΔI_o and verify that

$\Delta I_o < 0.3 I_o$

Table 3
Buck converter design parameters.

V_T	30
V_o	12
L	0,06
R_{eq}	1,2
f	3906,25
I_o	10

Table 4
Buck converter computed parameters.

D	0,4
ΔI_o	0,0307
Δv_c	1
C_{min}	9,830E-07
C_{max}	0,01042

c) Select a permissible value of ΔV_o
d) Compute value of $C_{\min}$ for the desired maximum output voltage rippleΔV_o.
e) Compute value of $C_{\max}$ to ensure overdamped inductor current response.
f) Select a convenient value of C such that

$C_{\min} \le C \le C_{\max}$

g) Repeat computations for the expected range of variation of V_o,I_o,V_T, to find values of L and C that work satisfactorily in all cases.

Let us consider for example the following design parameter specifications given in Table 3.

Using formula (8) through (12) we compute the following results given in Table 4.

Table 5 shows final capacitor value selected, and the resulting expected voltage ripple.

Buck converter experimental results

Shown in Fig. 16 is the oscilloscope screen output of the battery current and pulse width modulation in the buck converter built and tested.

Battery charging

For energy storage purposes, a bank of batteries is used. These must be charged according to a specified cycle for better efficiency and life expectancy. Two types of batteries are preferred in this application: deep cycle and Lithium based (such as LiFePo). The first type is the most commonly found given its lower price range. However, they are less efficient, have lower life expectancy, and are much heavier.

In the case of deep cycle batteries there are generally 3 charge stages (Trojan Co., 2016):

a) Bulk charging
In this stage, the SOC (State of Charge) is at its lowest, i.e. the battery voltage is at its lowest. The battery is charged at the highest current rate allowable, as specified by the manufacturer, until the voltage battery reaches a first threshold value ($V_{bulk\ regulation}$). The charging voltage can be very high as long as the charging current remains below a specified limit (I_{bulk}).
b) Absorption
In this stage, the battery is charged at a constant voltage ($V_{absorption}$), which is only slightly higher than its nominal value. This charging voltage is maintained as long as the battery maintains its voltage within range. This ensures that the battery charges to its full capacity. When the voltage reaches its second threshold voltage it is said to be in full SOC.

Table 5
Buck converter selected value results.

$C_{selected}$	1,00E-06
Δv_c	9,83E-01

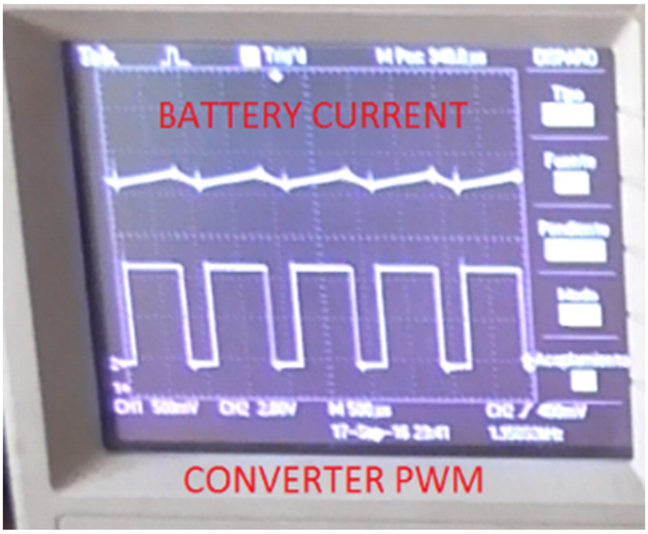

Fig. 16. Operational variables behavior in buck converter.

c) Floating
This stage is necessary for compensating natural discharge of the battery, thus maintaining 100% SOC before using.

Fig. 17 shows a short sequence of charge/discharge cycles on an Ultracell battery (12 V, 1.3 AH) using our programmable buck converter design. Being configurable is a powerful feature of the proposed solution since any given battery can be charged according to the manufacturer's recommendations. The charging setup entered to the Arduino in this case is given in Table 6. The Arduino program controls the duty-cycle percentage so the charging cycle follows Table 6, measuring from available sensors the input voltage, output voltage, and output current as depicted in Fig. 14.

Table 6
Test Charging Setup.

Parameter Setup	Value
Max Voltage in bulk mode [V]	16.0
Max Current in bulk mode [A]	2.0
Absorption Voltage [V]	14.4
Floating Voltage [V]	13.8

Field test results

This section presents evidence of the successful application of the proposed configuration of generator and buck converter with different prime movers. The proposed architecture was used in the devices shown in Figs. 2–4. Selected field results are shown next for illustrative purposes.

Tidal turbine

Insight into the suitability of a generator for a given rotor can be gained by examining the speed versus torque curve. Other important curves such as the speed versus power and Cp versus TSR can be derived from it.

The generator and buck converter were connected to the tidal turbine shown in Fig. 4. Torque and RPM data were obtained by varying the resistive load on the generator, which was previously calibrated. Fig. 18 shows field test results.

In the range of torque and speed tested, as the torque increases, the speed slightly decreases. This somewhat linear behavior is expected until the output torque approaches the maximum torque. Then the speed will begin to decrease abruptly before stalling. This characteristic was predicted by TURBEM. However, the actual measurements of the complete system are approximately 30% lower. This difference can be explained by inaccuracies resulting from the fluid mechanics model idealization as well as mechanical losses due to friction not being modeled. Tip and hub losses may be higher than predicted by the Prandtl factor due to short blades and

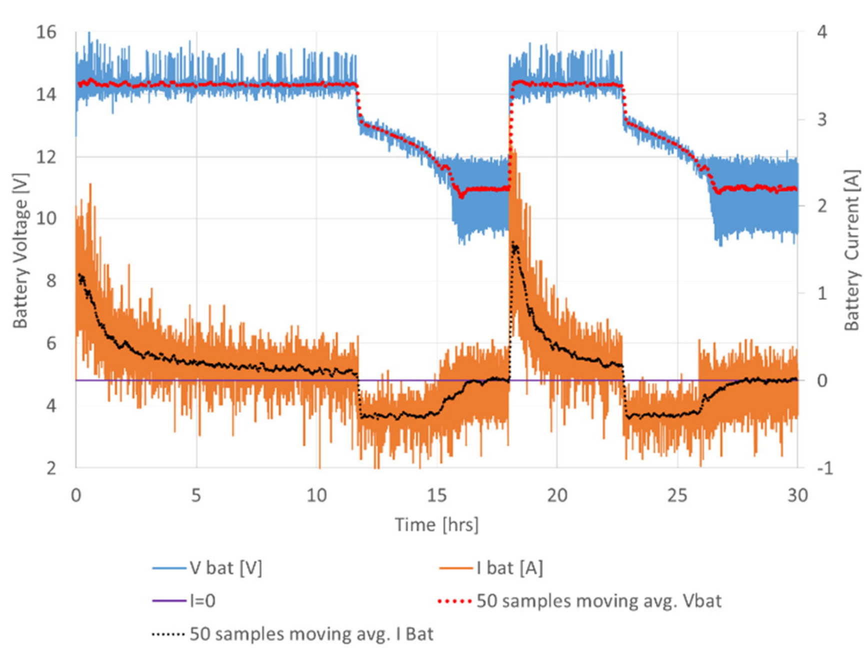

Fig. 17. Trial Charge/Discharge cycles.

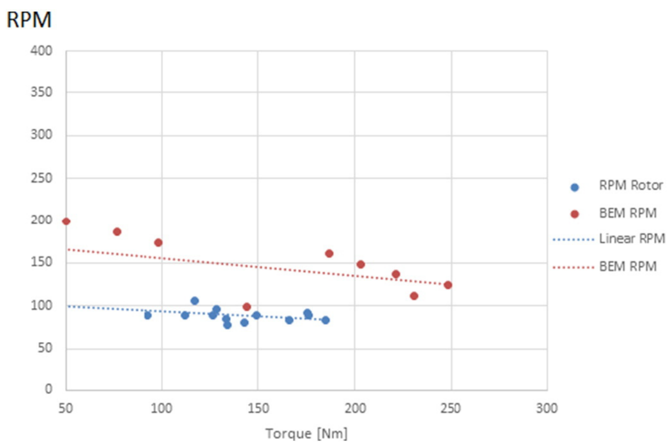

Fig. 18. Rotor angular velocity (RPM) for 2 m/s upstream velocity. Experimental (blue orbelow) vs BEM predicted values (red or above) for Tidal Turbine. (For interpretation of the references to colour in this figure legend, the reader is referred to the web version of this article.)

relatively large chord lengths occurring in small size rotors such as in this case.

Wind turbine

Next shown in Figs. 19 and 20 are field test results for the wind turbine of Fig. 3 that uses the proposed configuration and design methodology.

Fig. 19 contains the information necessary to generate the experimental C_P vs TSR of Fig. 20 usually used for benchmarking wind turbines. The values as predicted by TURBEM are included in Fig. 20 for comparison.

The actual system output is less than the theoretically predicted but nevertheless with an accuracy in the order of 30% to 50%. However from the design point of view, the proposed configuration of generator andbuck converter works quite as expected. The difference between predicted and measured values of the complete system should be attributed mostly to the shortcomings of the BEM theory, in which TURBEM 2.0 is based, as well as unmodeled aspects such as dry friction.

The wavy nature of the theoretical C_p curves that is observed in Fig. 20 can be explained due to the nature of the BEM equations. In TURBEM (Chiang, 2016a) these equations are solved numerically. At higher values of TSR, the convergence rate is unsteady. Hence the accuracy of root finding of the induction factors (a and a′), with which the performance of the turbine is estimated, is diminished.

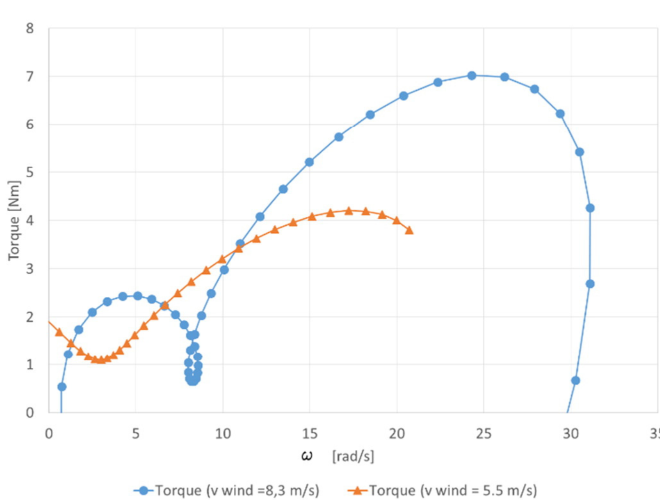

Fig. 19. ω vs Torque curves of a small wind turbine using the proposed configuration. The lobe in the 8.3 m/s curve is due to polynomial curve fitting of the method used to derive these curves.

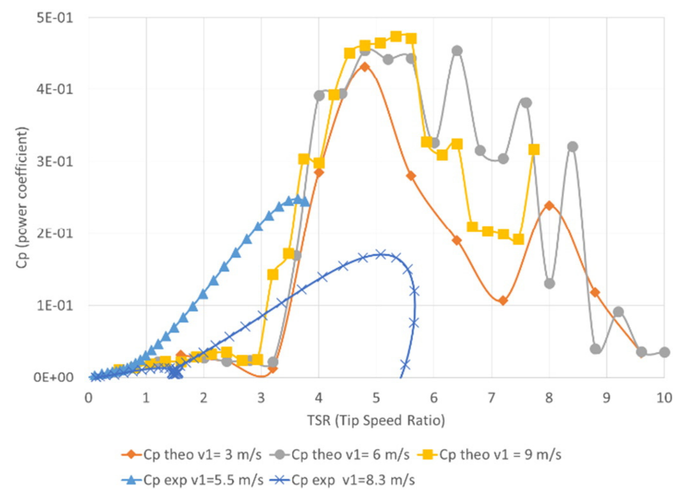

Fig. 20. Power Output Results. Theoretical vs field tests. The final output is around 50% relative to wind rotor because of internal friction and ohmic losses in the generator and buck converter. For this scale it is an acceptable output.

Conclusions

An effective architecture for power management of small scale NCRE converters applicable to multiple primary energy sources is proposed and evaluated. The proposed design configuration is an improvement in reliability and cost effectiveness since the following criteria guide the design process: a)low cost materials, b)simple manufacturing methods, and c)simplified design methods. The purpose of the design is to store electric energy in a battery bank for use when needed.

The design configuration consists in the following building blocks described in this article: a)3 phase axial flow permanent magnet generator, b)3 phase AC to DC bridge rectifier, c)programmable buck converter (MPPT), and d)battery bank. The application is enhanced by optimal compatibility of the output of the generator with the charging cycle of the battery bank, for which the configurable buck converter is used. The design is customizable for different sets of design specifications using the simplified methods described herein. The validity of the design methodology has been corroborated experimentally. Given the design flexibility of this configuration, it can be used with small scale energy converters exploiting multiple NCRE sources.

Future work will consist in further improving the devices in terms of efficiency, cost, and reliability. An aspect of particular interest is the introduction of On Board Diagnostic (OBD) systems which can be added to each system to monitor their condition during operation, thus helping to prevent failure in a timely manner. One of the main drawbacks of small-scale energy devices is poor reliability, and our future aim is to work to develop better solutions taking advantage that components such as the MPPT in our proposed configuration contain integrated microcontroller and sensors that can be used in dual purpose for condition monitoring.

Appendix A. Supplementary data

Supplementary data to this article can be found online at https://doi.org/10.1016/j.esd.2017.09.001.

References

Anyi M, Kirke B. Hydrokinetic turbine blades: design and local construction techniques for remote communities. Energy for sustainable development, vol. 15, Issue 3. Elsevier; 2011. p. 223–30.

Aquatera. Aquatera, “recommendations for Chile's marine energy strategy: a roadmap for development”, Foreign and Commonwealth Office, UK. [Online] Available at: https://www.gov.uk/government/publications/recommendationsfor-chiles-marine-energy-strategy, 2014. [accessed 28-11-2016].
Arduino, “Arduino Uno 1”, Retrieved from https://www.arduino.cc/en/Guide/Introduction, 2016a, [accessed 28-11-2016].
Arduino, “Arduino Uno 2”, PWM frequency, Retrieved from http://playground.arduino.cc/Code/PwmFrequency, 2016b, [accessed 25-11-2016].
Arrau, J. F. (2016), “Diseño del generador de una turbina hidrocinética de pequeña escala, (Master's thesis), Department of Mechanical and Metallurgical Engineering, P. Catholic University of Chile, Santiago, Chile.
Ashuri T, Zaaijer MB, Martins JRRA, Van Bussel GJW, Van Kuik GAM. Multidisciplinary design optimization of offshore wind turbines for minimum levelized cost of energy. Renewable energy, vol. 68. Elsevier; 2014. p. 893–905.
Beaudin M, Zareipour H, Schellenberglabe A, Rosehart W. Energy storage for mitigating the variability of renewable electricity sources: an updated review. Energy for sustainable development, volume 22. Elsevier; 2010. p. 302–14.
Bhende CN, Mishra S, Malla SG. Permanent magnet synchronous generator-based standalone wind energy supply system. IEEE Trans Sustainable Energy Oct 2011; 2(4):361–73.
Bumby JR, Martin R. Axial-fluxpermanent-magnetair-cored generator for small-scale wind turbines. IEE Proc Electr Power Appl 2005;152(5):1065–75.
Chiang LE. Turbem 2.0 [computer software]. Santiago, Chile. Available from www.mecatronix.cl, 2016.
Chiang LE. “Sistemas Electromecánicos”, class notes. Department of Mechanical and Metallurgical Engineering, P. Catholic University of Chile; 2016b.
Chiang-Sánchez, Luciano (2012), “Boya Mecatrónica” (Mechatronical Heaving Buoy) N/Ref.: PAT 2724/2012, Pontificia Universidad Católica de Chile, Invention Patent, Chile.
Drew B, Plummer AR, Sahinkaya MN. A review of wave energy converter technology. Proc IMechE A J Power Energy 2009;223:887–902.
Falcao Antonio. Wave energy utilization: a review of the technologies. Renew Sustain Energy Rev 2010;14:899–918.
Gitano-Briggs H. Small wind turbine power controllers, wind power. In: Muyeen SM, editor. InTech 978-953-7619-81-7; 2010. Available from: http://www.intechopen.com/books/wind-power/small-wind-turbinepower-controllers. [accessed 20-11-2016].
Hansen M. Aerodynamics of wind turbines. Taylor & Francis; 2015.
Hiremath RB, Kumar B, Balachandra P, Ravindranath NH, Raghunandan BN. Decentralised renewable energy: Scope, relevance and applications in the Indian context. Energy for sustainable development, volume 13. Elsevier; 2009. p. 4–10.
Holmes AS, Hong G, Pullen KR. Axial-flux permanent magnet machines for micropower generation. J Microelectromech Syst 2005;14(1):54–62.
Lago LI, Ponta FL, Chen L. Advances and trends in hydrokinetic turbine. Energy for sustainable development, volume 14. Elsevier; 2010. p. 287–96.
Lázaro-Blanco A, Barrado-Bautista A. Problemas de Electrónica de Potencia. Ch.5 Madrid: Pearson/Prentice-Hall; 2007.
Louie H. Experiences in the construction of open source low technology off-grid wind turbines. IEEE PES General Meeting, Detroit, MI, USA, 2011. ; 2011.
Louie H, Szablya S. Electromagnetic field modeling of appropriate technology generators for rural electrification applications. IEEE GHTC, Seattle, WA, Oct 2011; 2011.
Louie H, Vincent Van Acker V, Szablya S, Dauenhauer P. Opportunities and challenges formicro wind turbines in developing communities. IEEE global humanitarian technology conference Seattle, WA, USA, Oct. 2012; 2012.
Maalawi KY, Badr MA. A practical approach for selecting optimum wind rotors. Renew Energy, Pergamon 2003;28:803–22.
Muñoz AH, Chiang LE, De La Jara EA. A design tool and fabrication guidelines for small lowcost horizontal axis hydrokinetic turbines. Energy for sustainable development, volume 22. Elsevier; October 2014. p. 21–33.
Palit D, Chaurey A. Off-grid rural electrification experiences from South Asia: status andbest practices. Energy for sustainable development, volume 15. Elsevier; 2011. p. 266–76.
Probst O, Martínez J, Elizondo J, Monroy O. Small wind turbine technology, wind turbines. In: Al-Bahadly Dr Ibrahim, editor. InTech; 2011. https://doi.org/10.5772/15861. Available from: https://www.intechopen.com/books/wind-turbines/small-wind-turbine-technology. [accessed 06-04-2017].
Rodriguez J, Burgos J, Arnatte S. Sistemas Eólicos de Producción de Energía Eléctrica. Madrid: Rueda S.L; 2003.
Topaloglu I, Nakanishi Y, Korkmaz F, Nakashima Y. Axial flux permanent magnet generator with low cogging torque for maintenance free under water power generating system. Int J Renew Energy Res 2016;6(2):510–9.
Trojan Battery Company. User's Guide, s.l.: s.n. Retrieved from www.trojanbattery.com, 2016. [accessed 15–11-2016].
Vansompel H, Sergeant P, Dupre L. Optimized design considering the mass influence of anaxial flux permanent-magnet synchronous generator with concentrated pole windings. IEEE Trans Magn 2010;46(12):4101–7.